vices, such as teletypewriters and the CDC-274 Digigraphics or the IBM-2250 Graphics consoles.

References

[1] Dethlefsen, D. G., ed., "The Mission Analysis and Trajectory Simulation Program Engineering Document," Feb. 1967, TRW Systems Group, Redondo Beach, Calif.

[2] Lanzano, B. C., ed., "The Mission Analysis and Trajectory Simulation Program Programmer's Handbook," and "The Mission Analysis and Trajectory Simulation Program User's Guide," both rev. Jan. 1970, TRW Systems Group, Redondo Beach, Calif.

Interaction of Gases with an Ablator and the Ablator Components

FRANK I. AKERS,* WAYNE H. GRIEST,* RUSSELL K. LENGEL,* AND JAMES P. WIGHTMAN†
Virginia Polytechnic Institute, Blacksburg, Va.

THE interaction of gases with a "discontinuously filled elastomer" (a material consisting of a matrix in which colloidal sized particulate matter is dispersed) has both theoretical and applied significance. For example, a 15% vacuum-induced decrease in the thermal conductivity of an ablator has been reported[1] and re-exposure of the ablator to the atmosphere for 24 hr caused the thermal conductivity to revert to substantially its pre-exposure value. These results suggest that gas sorption-desorption may be partially reponsible for the observed changes in thermal conductivity. One purpose of the present work was to measure quantitatively the amounts of several gases sorbed by the same ablator used in the thermal conductivity studies.

The mechanism of sorption of each gas on the ablator is of intrest also. However, since the ablator is a composite material it is not possible from sorption measurements on the ablator itself to define unambiguously the sorption mechanism. A knowledge of which component the gas is interacting with is a necessary step in defining the mechanism. A second purpose of this Note is to present the results of sorption studies on the individual components of the ablator to elucidate the sorption mechanism.

Materials and Experimental Procedures

The ablator used was a filled silicone elastomer designated NASA E4A1 with the following composition: silicone elastomer (73 wt%), silica spheres (11 wt%), phenolic spheres (10 wt%), and silica fibers (4 wt%). The matrix was prepared at the NASA-Langley Research Center using GE silicone liquid (RTV-602). The silica spheres were Eccospheres SI manufactured by Emerson and Cuming, Inc.; these hollow microspheres had a particle size range of 30 to 125μ and a wall thickness of $\sim 2\mu$. The hollow phenolic shperes (#BJO-0930) were Microballons manufactured by Union Carbide Corporation from Bakelite phenolic resin and had a particle size range of 5 to 127μ. The silica fibers (J-M: 110) were microquartz fibers of $\sim 2\mu$ diameter manufactured by Johns-Manville.

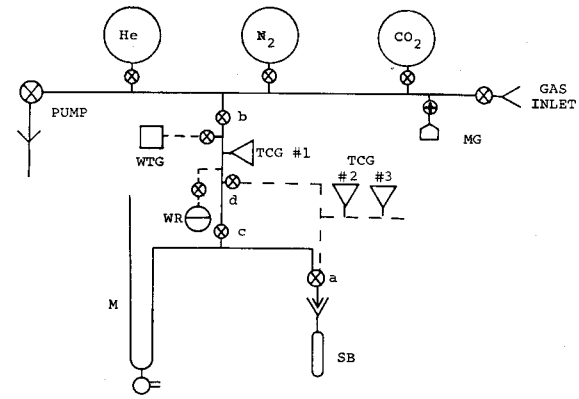

Fig. 1 Apparatus for the determination of gas sorption.

The sorption of various gases at room temperature by the ablator was measured in the constant-volume apparatus shown in Fig. 1. The test sample consisting of about 34 cubes ($\sim$5 mm on edge) of the ablator weighing 3.4555 g in sample bulb SB were evacuated in a liquid nitrogen trapped mercury diffusion pump system to $<1 \times 10^{-5}$ torr at room temperature and stopcock a closed. A volume of test gas was introduced via stopcocks b and c. Stopcock c was then closed, and the gas pressure was read on the Hg manometer M. Stopcock a was then opened, the gas was expanded into SB, and the pressure decay $p(t)$ was recorded until dp/dt was $\sim$0.02 torr/min over a 30-min period. The sample was evacuated at room temperature to $<1 \times 10^{-5}$ torr as read on McLeod gauge MG after each gas exposure. Sorption measurements were made at 50°C by immersion of SB into a constant-temperature water bath.

The procedure for water sorption was modified as follows: water vapor was introduced from the water reservoir WR.

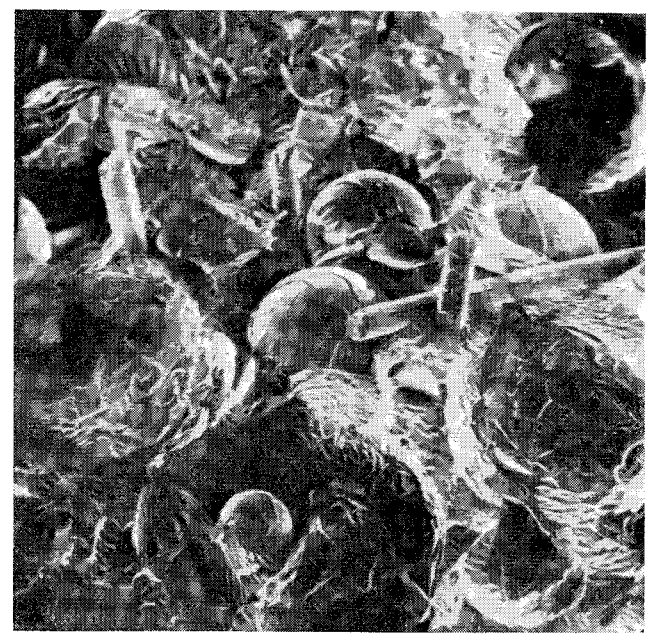

Fig. 2 Stereoscan micrograph of NASA ablator E4A1.

Received April 22, 1970; revision received May 27, 1970. Supported under NASA-Langley Research Center Contract NAS1-7645. Results on ablator presented in part before the Division of Colloid and Surface Chemistry at the 156th National American Chemical Society Meeting, Atlantic City, N.J., September 1968; results on ablator components presented in part at Virginia Academy of Science, Fredricksburg, Va., May 1969. The authors wish to express their appreciation to R. G. Saache, Department of Dairy Science, VPI, for his help in obtaining light microphotographs. The scanning electron photographs were obtained for the authors by the Monsanto/Washington University ONR/ARPA Association, St. Louis, Mo.

* Research Assistant, Chemistry Department.
† Associate Professor, Chemistry Department.

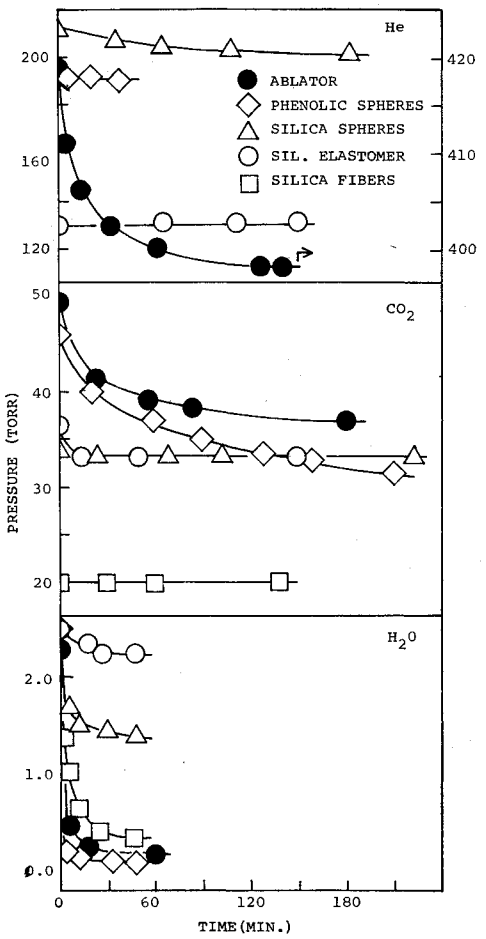

Fig. 3 Pressure-time plots for sorption on ablator E4A1 and components.

The pressure was measured on the thermocouple gauges TCG-1 and TCG-2 (0-20 torr). Stopcock a was then opened and water vapor expanded into SB; $p(t)$ was measured using thermocouple gauges TCG-2 and TCG-3 (0-1 torr). Final pressures were taken 60 min after expansion. All thermocouple gauges were calibrated for water using a Wallace-Tiernan absolute pressure gauge WTG (0-20 torr). The effect of water vapor adsorption on the glass walls was determined by expanding through stopcock d into the previously evacuated volume between stopcocks a and d.

A gravimetric procedure was used to determine water sorption at $p > 0.4$ torr, where it was not feasible to use the expansion technique. A cylindrical sample (5 mm × 35 mm) weighing 0.5106 g was suspended from a Worden quartz spring having a spring constant of 2.0×10^{-3} g/mm. Spring elongation was followed with a traveling microscope. The sample was evacuated at room temperature to $<1 \times 10^{-5}$ torr and a microscope reading was taken. Water vapor was introduced, and a reading was taken 30 min later. The water vapor pressure was increased and a reading was taken again after 30 min. This procedure was repeated over a 3-hr period. Water vapor pressures were read on a thermocouple gauge. In a different series of water measurements, microscope readings were taken 5 min after introduction of the water vapor; the sample was then evacuated at room temperature to $<1 \times 10^{-3}$ torr between each exposure.

Table 1 Sorption parameters for gases on NASA ablator E4A1

Gas	T, °C	ΔN, moles/g-torr ($\times 10^8$)
N_2	27.9	0.723
N_2	49.1	0.900
He	27.4	1.59
He	48.5	1.89
CO_2	27.1	14.6
CO_2	48.9	10.1
H_2O	27.5	6660.0[a]
H_2O	48.8	3000.0[a]

[a] Initial slope.

The same apparatus and procedure were used for sorption measurements at 27°C on the following quantities of the components: silica spheres, 0.381 g; silica fibers, 0.138 g; silicone elastomer, 2.526 g; phenolic spheres, 0.346 g. These proportions correspond to the ablator composition.

Sorption by Ablator

The random distribution of both spheres with diameters ranging from 20 to 40μ and fibers in the matrix of the ablator is shown in a microphotograph obtained with a scanning electron microscope (Fig. 2). Several fibers are seen perpendicular to, while another fiber is essentially parallel to, the fracture surface.

Typical $p(t)$ plots obtained on exposure of the ablator to He, CO_2, and H_2O are shown by the closed points in Fig. 3. The time required to saturate the ablator with He or CO_2 (or N_2, not shown) was on the order of 2–4 hr, whereas for H_2O 90% of the vapor pressure decrease occurred in 5 min.

The decrease in pressure Δp in a constant-volume system is related to the amount of gas (Δn) sorbed by the ablator by

$$\Delta n = (\Delta p)V/W_sRT \qquad (1)$$

Where V is the system volume, W_s is the weight of the ablator,

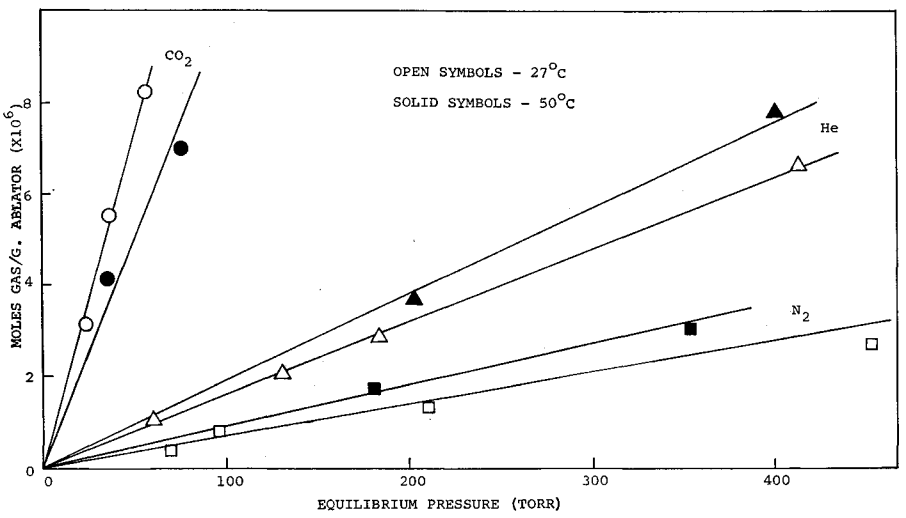

Fig. 4 Gas sorption on ablator E4A1 as a function of pressure.

Table 2 Comparison of component and composite sorption on NASA ablator E4A1

Gas	Component	ΔP, torr	V, cc	ΔN, moles g^{-1} ($\times 10^6$)	P_{eq}, torr
He	Silica spheres	12.0	13.7	2.52	200.0
He	Phenolic spheres	2.1	15.4	0.50	192.0
			Sum =	3.02	
			Composite =	3.10	200.0
CO_2	Phenolic spheres	13.9	14.8	3.16	32.2
CO_2	Silicone elastomer	3.4	22.9	1.19	33.0
			Sum =	4.35	
			Composite =	4.30	33.0
H_2O	Phenolic spheres	2.78	264	11.6	0.067
H_2O	Silica fibers	2.63	264	10.9	0.22
H_2O	Silica spheres	1.50	264	6.2	1.35

R is the gas constant, and T is the temperature. Figure 4 shows linear relationships for Δn vs saturation pressure for N_2 He, and CO_2; the sorptions of He and N_2 vary directly with temperature, whereas the sorption of CO_2 varies inversely.

The sorption of H_2O, shown in Fig. 5, is much greater than that of CO_2, although the temperature dependence is in the same direction. Table 1 lists the slopes from Figs. 4 and 5 for each gas at each temperature. The sorptions of N_2 and CO_2 differ by a factor of ~20, whereas the sorption of H_2O is some 450 times larger than CO_2.

The type of interaction occurring between CO_2, He, and N_2 and the ablator is not obvious from the experimental results. On the other hand, the sorption of water was defined in an additional series of experiments as previously noted. The results are shown in Fig. 6. Brunauer has classified isotherms for the adsorption of gases on solids according to shape.[2] The top curve in Fig.6 suggests type II adsorption behavior; however, the convex portion occurs at the rather low value of ~0.3 for p/p_o, the ratio of the saturation pressure to the vapor pressure of water at 27°C. Hence, the experiment was repeated but allowing only 5 min for equilibration and with evacuation between doses, and the bottom curve reflects adsorption of water by the ablative material, that is, interaction of water with the surface and not the bulk of the ablator. Recall that the pressure-time plots for water fell abruptly and were essentially complete in 10 min contrasted to the other gases. This is consistent with physisorption where gases may be adsorbed rapidly, as determined in part by the number of collisions with the surface. A BET analysis[3] of

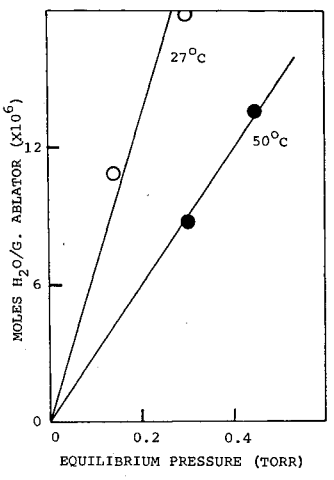

Fig. 5 Sorption of H_2O by ablator E4A1 as a function of pressure.

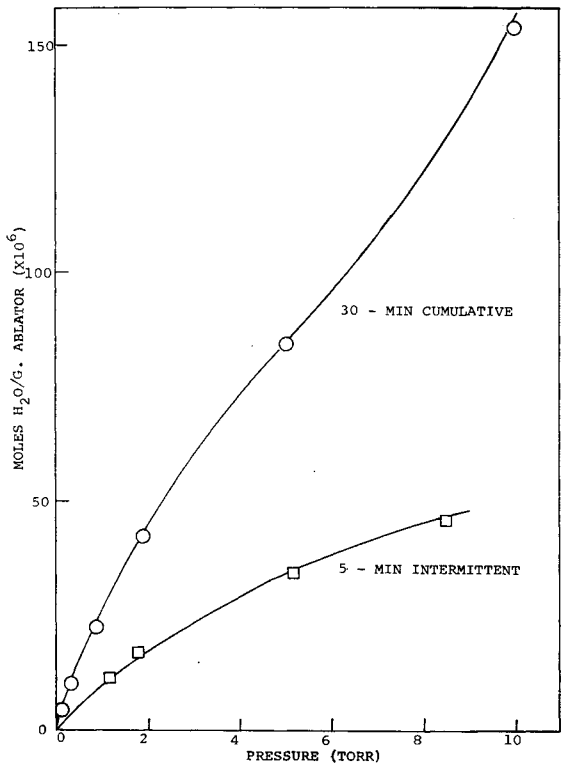

Fig. 6 Sorption of H_2O by ablator E4A1 at 27°C as a function of pressure.

the data shown in the bottom curve in Fig. 6 gave a surface area of the ablative material of 1.6 m^2/g. The upper curve thus represents rapid adsorption plus a slower sorption by as yet an unspecified mechanism.

Sorption by Ablator Components

Figure 3 includes plots for the sorption of He, CO_2, and H_2O on the components of the ablator. For He, the most significant interaction occurred with the silica spheres, and negligible interaction occurred between He and the silicone

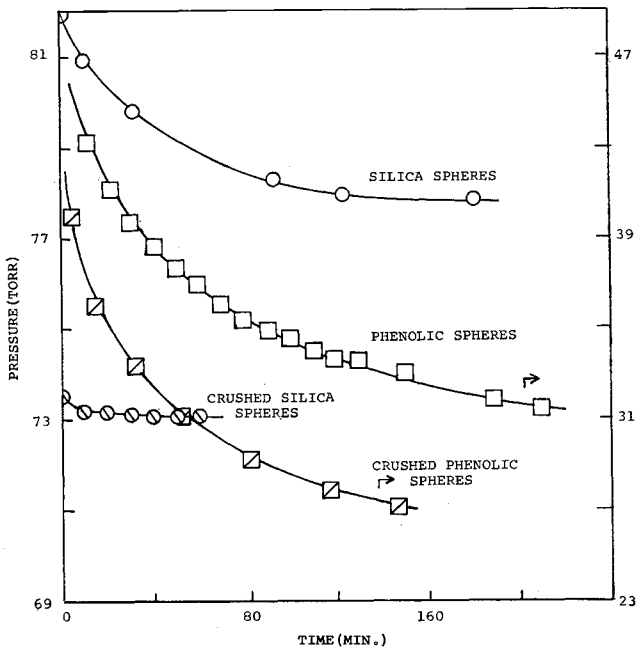

Fig. 7 Pressure-time plots on exposure of silica spheres and phenolic spheres to CO_2 at 27°C.

elastomer. For CO_2, predominant sorption was noted with the phenolic spheres. For H_2O, a major interaction also occurred with the phenolic spheres, and it was much more rapid (< 10 min, compared with 3–4 hr for CO_2). The silica fibers sorbed water more slowly than did the phenolic spheres, but they sorbed about the same amount of H_2O.

Component and composite sorption are compared in Table 2. Approximately 85% of the total He sorbed is due to interaction of He with the silica spheres, and the balance, with the phenolic spheres. The saturation pressure obviously must be about the same in the two cases in order to make valid comparisons. The question arises: can the sorption of a given gas by the ablator be treated as a simple sum of the sorption by the components? Interpolation of the results in Fig. 4 gives 3.10×10^{-6} moles of He sorbed per gram of ablator at 200 torr. It is significant that the sum of the component interactions is in excellent agreement with this value as shown in Table 2. Similar agreement with respect to the additivity principle is seen for CO_2. For H_2O sorption, however, comparisons of either the extent of component interactions or of the component interactions with the ablator are not possible, since it is experimentally difficult to adjust initial pressures in the technique used such that equivalent saturation pressures are obtained.

The mechanism of He interaction with the silica spheres, and of CO_2 with phenolic spheres, were demonstrated in additional experiments in which crushed silica and phenolic spheres, respectively, were used. Sorption of He on the crushed glass spheres was negligible (Fig. 7). The mechanism of He sorption on the silica spheres then involves simply the diffusion of He through the walls. The diffusion of He through glass is a well-documented phenomenon.[4] The story is different for CO_2 and the crushed and uncrushed phenolic spheres, also shown in Fig. 7. The two curves may approach the same limit at long time, but over 2–3 hr the sorption of CO_2 on crushed phenolic spheres is greater than on the uncrushed phenolic spheres; hence the CO_2 must interact with the bulk phenolic resin represented by the annuli of the hollow spheres. However, diffusion of CO_2 does occur from the interface to the bulk resin and hence the long time necessary to saturate the sample. We have indeed shown[5] that it is possible to obtain the infrared spectrum of the sorbed CO_2 in the phenolic resin. The interaction of CO_2 with the silicone elastomer was not established.

The mechanism of water interaction with the phenolic spheres, silica fibers and silica spheres was not unambiguously established. However, the rapid decrease in water vapor pressure on exposure to the phenolic spheres suggests physisorption of water. The somewhat slower decrease in water vapor pressure on exposure to the silica fibers may be due to physisorption in the small pores of the silica fibers. The different amounts of water sorbed by the ablator at 5- and 30-min intervals are consistent with the time difference observed in the case of the phenolic spheres and the silica fibers.

References

[1] Mugler, J. P., Jr. et al., "In Situ Vacuum Testing—A Must for Certain Elastomeric Materials," *Journal of Spacecraft and Rockets*, Vol. 6, No. 2, Feb. 1969, pp. 219–221.

[2] Brunauer, S., *The Adsorption of Gases and Vapors*, Princeton Univ. Press, Princeton, N.J., 1945, pp. 14–19.

[3] Orr, C. Jr. and Dallavalle, J. M., *Fine Particle Measurement: Size, Surface and Pore Volume*, Macmillan, New York, 1959, pp. 198–200.

[4] Dushman, S., *Scientific Foundations of Vacuum Technique*, 2nd ed., Wiley, New York, 1962, p. 676.

[5] Akers, F. I. and Wightman, J. P., "Absorption of CO_2 by Phenolic Resin," *Journal of Applied Polymer Science*, Vol. 14, No. 1, Jan. 1970, pp. 241–243.

Scale Modeling Considerations for Thermal Control Coatings

R. K. MacGregor
Renton, Wash.

AND

R. K. Thompson*
University of Washington, Seattle, Wash.

Nomenclature

H,W = characteristic dimensions in the x and y directions
k = thermal conductivity
L = model scale ratio; e.g., $L = H_m/H_p$
q = heat transfer
R = thermal resistance
t = material thickness (z direction)
T = temperature
x,y,z = coordinate directions

Subscripts

c,s = coating and substrate, respectively
m,p = scale model and prototype, respectively

Introduction

EXTENSIVE studies into the development of scale modeling criteria and the application of scale modeling techniques to spacecraft systems have been presented.[1–4] Recent studies have delved into the limitations inherent in scale modeling due to material and gage availabilities and uncertainties in thermophysical properties.[5,6] These studies have pointed out certain problem areas in the application of scale modeling techniques. One problem, considered herein, relates to the thickness of the thermal control coatings that are used to control radiant heat transfer on the spacecraft. For most solar reflecting coatings, the thickness (typically 10 mils) must be maintained in order to preserve the radiative properties of the surface. In the scale models this preservation of coating thickness significantly affects the heat conduction balance. The temperature errors induced in scale models as a result of preserving the coating thickness and a technique for over-scaling the substrate to offset coating effects, are discussed in this Note.

Discussion

Consider a thermal control coating of thickness t_c applied to a substrate panel of dimension $H \times W \times t_s$, as measured in the x, y, and z directions, respectively. The thermal resistance for heat transfer normal to the substrate and coating (in the z direction) may be expressed as

$$R = (k_c t_s + k_s t_c)/t_c t_s HW \tag{1}$$

Ratioing the thermal resistance for a scale model to that of the prototype configuration results in the equation

$$R_m/R_p = (H_p W_p/H_m W_m)[t_{cp}t_{sp}/t_{cm}t_{sm}] \times [(k_{cm}t_{sm} + k_{sm}t_{cm})/(k_{cp}t_{sp} + k_{sp}t_{cp})] \tag{2}$$

If the model is constructed with rigid adherence to the three-dimensional scaling criteria as discussed in Refs. 1–5, where $L = H_m/H_p = W_m W_p = k_{sm}/k_{sp} = t_{sm}/t_{sp} = k_{cm}/k_{cp} = t_{cm}/t_{cp}$, then the ratio of thermal resistances reduces to

$$R_m/R_p = 1/L^2 \tag{3}$$

Received March 13, 1970; revision received May 11, 1970. Portions of the work presented here were performed for NASA-Marshall Space Flight Center under Contract NAS8-21422.

* Coordinator of Special Studies, Office of the Vice-President for Planning and Budgeting.